Implementation of a Transformer-Less Common Mode Active Filter for Off-Line Converter Systems

M. L. Heldwein[1], H. Ertl[2], J. Biela[1] and J. W. Kolar[1]

[1]Swiss Federal Institute of Technology (ETH) Zurich
Power Electronic Systems Laboratory
ETH Zentrum / ETL H23, Physikstrasse 3
CH-8092 Zurich / SWITZERLAND / Europe
heldwein@lem.ee.ethz.ch

[2]Technical University Vienna
Dept. of Electrical Drives and Machines
Power Electronics Section
Gusshausstrasse 27/372, A-1040 Vienna, Austria
j.ertl@tuwien.ac.at

Abstract — **This work presents a study and practical implementation of an active filter employing a HF power amplifier and passive filter components to be connected to the AC power lines in order to mitigate common mode conducted emissions of PWM converter systems. The filter topology is chosen from different possibilities listed in a literature survey and studied regarding practical implementation issues. Special attention is put on the stability analysis where the challenges for the feedback structure are discussed and a simple feedback structure is proposed. A prototype is designed and built, from which mathematical and experimental results are obtained demonstrating the potential and limitations of such a system.**

I. INTRODUCTION

In modern power electronic systems, volumetric densities are found usually in the 1 to 3 kW/dm^3 range, depending basically on the employed technology and switching frequency. For higher power densities higher switching frequencies are to be used but EMC filtering components are still responsible for a large volumetric occupation in the power system. In some cases the EMC filters represent more than 30% of the total power supply volume and even if lower switching frequencies are used, the occupation is no less than 10%. In a world where system and application space gets more and more expensive, the volumetric reduction of power supply components is of great importance. A proposed solution for the size reduction of EMC filters is the use of active systems [1-4], commonly called active filters, instead of fully passive filters. High frequency (HF) active filters are broadly employed in signal processing, where low current and voltage levels are present. But, as power levels increase, the construction of such systems becomes critical, once wide-band amplifiers are to be used, which should be able to handle high current and voltage levels. This challenge motivates research in this field and is addressed in the following.

The scope of this work is limited to the common mode (CM) conducted emissions mainly in the frequency range of 150 kHz to 30 MHz. The connection of the EMC filter to the power circuits is thought to be on the AC mains side where a large 50 or 60 Hz frequency component is present, along with its low frequency harmonic contents. In this application the main function of the filtering systems considered here is the reduction of high frequency CM emissions. For that, the filters are based on linear HF power amplifiers as switched circuits are currently not providing the required operating bandwidth. The reduction of CM emissions is an important issue in all fields of electronics applications. The traditional approach is the use of Y-rated capacitors in addition to CM inductors and in most applications the size of these capacitors is limited due to safety regulations restringing the earth leakage currents. A practical active filter should be able to meet all relevant safety and EMC regulations, as well as high voltage surge requirements, and the filter stability should be independent from the impedances it is connected to. Costs are also a limiting factor and should not be higher than those for a conventional passive system.

From the potential advantages of the use of active filter circuits for reducing high frequency conducted emissions in power electronic
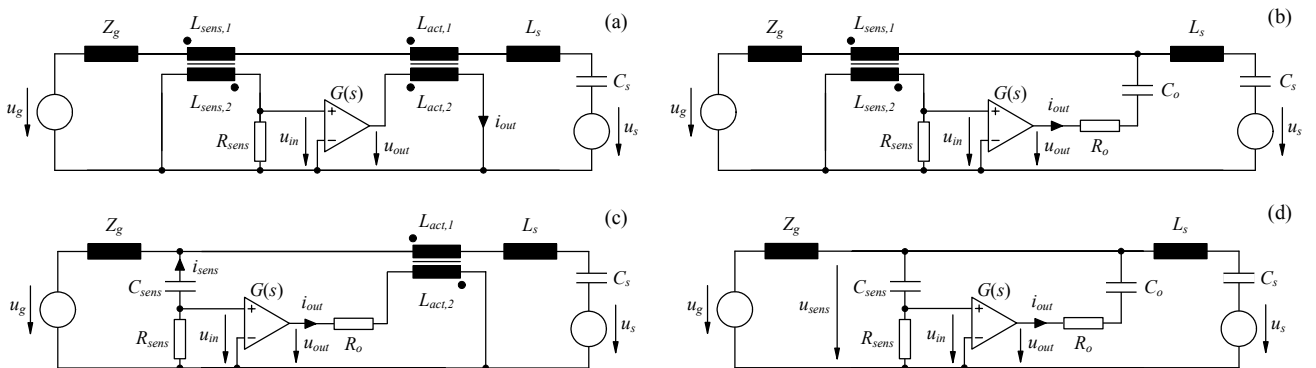

Fig.1: Basic active filter structures in their single phase equivalent circuits. The noise source is modeled as a voltage source in series with a capacitor C_s and an inductor L_s. The mains impedance Z_g is considered inductive.
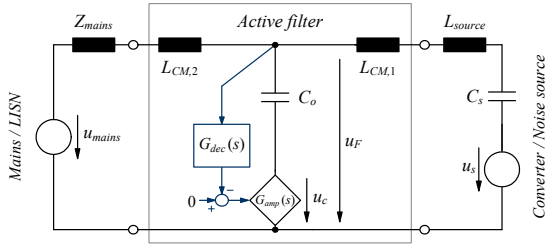
Fig.2: Simplified single-phase schematic showing the basic principle of the selected CM filtering system.

circuits, the search for a feasible and reliable system is a logical step. For the design of an active EMC filter the knowledge about the different possible structures is essential. Basically four types of circuits [2] are cited in the literature and shown in **Fig.1** as simplified single phase equivalent circuits. The basic division into four circuits is taken due the types of parameters that are used in the measurement and in the actuation paths. The basic strategies rely on the measurement of either current (Fig.1(a), [3-5] and Fig.1(b), [6-8]) or voltage (Fig.1(c), [9-10] and Fig.1(d), [11-14]), and in the injection of a shunt current (Fig.1(b) and Fig.1(d)) or a series voltage (Fig.1(a) and Fig.1(c)) to the AC lines. Besides the topologies of Fig.1 other active filter structures using a combination of the shown circuits can be applied [15-18], e.g. by using a current measurement feedback together with a voltage measurement feed-forward. The placement of an active filter actuator can also vary, i.e. the filter could be placed at the converter output and/or DC-link, directly in the AC input lines or mixing two of these [18].
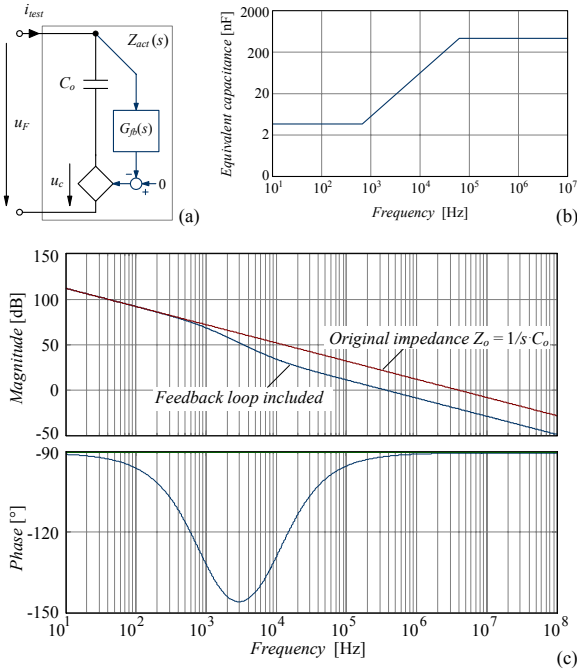

Fig.3: Basic principle of an active filter with capacitive coupling. **(a)** Impedance Z_{act} of a capacitor with a voltage feedback loop. **(b)** The equivalent capacitance is increased in the higher frequencies through the active feedback action. **(c)** Example of impedance curves $Z_{act}(f)$ illustrating the feedback action.

In this paper a filter topology to be placed in the AC lines comprising a capacitive coupling actuation and a voltage measurement according to Fig.1(d) is studied. The active filter structure is well known [11-14], therefore the emphasis is placed on the design of the feedback loop since it will decide on the system stability and on challenges of the practical construction. The use of an active feedback can lead a passive system to unstable operating modes and for the case at hand a stability analysis is addressed. As will be seen the proper placement of zeros and poles in the feedback path is of high importance [4], [11]. The theoretical basis for the determination of zeros and poles will be presented, along with results obtained from a first prototype relying on the described theoretical analysis.

The paper is framed as follows. In **Section II** the chosen active filter topology and its basic operating principle are explained, while in **Section III** a discussion about the theoretical implementation of the active filter ensuring stability is carried out and the proposed feedback structure is presented. **Section IV** addresses the practical realization of the feedback structure in an active filter prototype, presenting simulation results along with experimental measurements. Conclusions and an outlook on future research are given in a final section.

II. SELECTION OF ACTIVE FILTER TOPOLOGY AND ITS BASIC OPERATING PRINCIPLE

By considering the circuits of Fig.1 one realizes that the noise source (C_s and L_s) and the power grid impedances (Z_g) are usually difficult to predict and/or control [19-20] but should obviously be included in the stability consideration. For the topologies making use of a line current based feedback or actuation employing current transformers, it could be harder to decouple the system stability from the source and grid impedances, since these are placed directly in series with the transformer changing its frequency behavior in a sensitive way. Another difficult issue is that the current transformer would need a large bandwidth and the simple inclusion of an extra winding in a conventional CM inductor would probably not guarantee a good high frequency magnetic coupling due to construction safety demands and the poor HF relative permeability characteristics of conventionally used materials. Besides that, self resonances due the magnetic materials are to be expected as well as winding capacitances. For these reasons the cost of a good HF current transformer would have to be added to the filtering system. Therefore, a topology based on capacitive measurement of the line voltage and utilizing also capacitors in the actuator stage seems to be a good choice for active filtering connected to the AC lines. The filter topology that is treated in this work is presented in the simplified schematics of **Fig.2**, corresponding to the circuit of Fig.1(d).

This topology is comprised of two common mode inductors ($L_{CM,1}$, $L_{CM,2}$), one coupling capacitor (C_o), a measurement path (G_{dec}) including a low frequency attenuation network for rejection of any unwanted high amplitude frequency components and an actuator, which is realized with a linear HF power amplifier (G_{amp}). This structure presents some advantages such as:

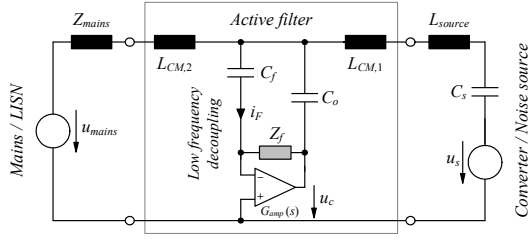- The filter structure and its principle are simple, presenting a po-

Fig.4: Basic single-phase equivalent circuit for the active filter including an amplifier G_{amp} and showing the variables of interest i_F and u_c.

tentially high stability range, increasing the possible filter attenuation in the frequency band of interest;

- Both, measurement (G_{dec}) and output coupling (through C_o) can be performed through Y-rated capacitors;
- As the needed inductance and capacitance values decrease by the use of an active feedback, better high frequency performance is to be expected than in a non-active filter, as smaller components usually present higher resonance frequencies;
- The implementation is potentially safe since the feedback measurement is done with low voltages; only a single HF power amplifier needs to be employed.

The use of the topology presented in Fig.2 has as main advantage the use of two inductors ($L_{CM,1}$, $L_{CM,2}$) and one capacitor (C_o) which are usually already present in any CM filter. For the case of CM noise filtering, these components are common mode chokes and Y-capacitors which technology is well know and won't make the filter more expensive. Since Y-capacitors have their values limited due to the safety limitation of the allowable earth leakage currents, the main idea with this active filter topology is to use the already employed
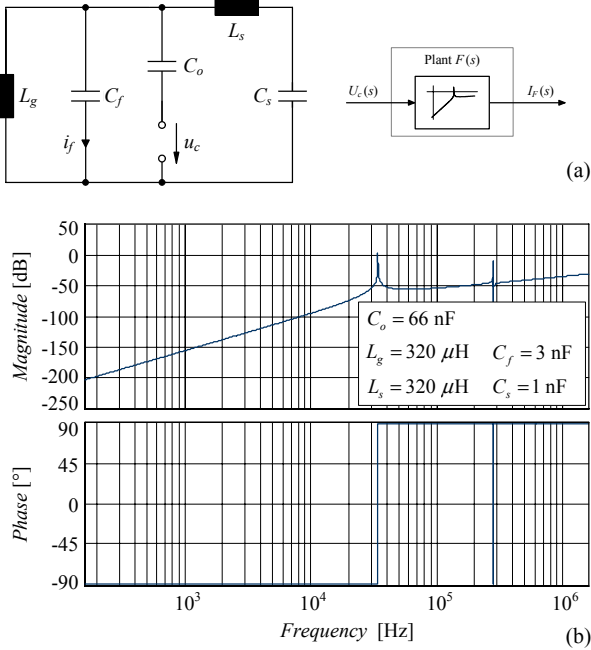

Fig.5: Circuit used for the stability analysis. Shown are **(a)** the basic circuit of the analyzed active filter plant with its transfer function and **(b)** an example of bode plots for an analyzed active filter plant.

values of Y-capacitors and allow for a noticeable reduction in the values of the inductors, which are usually large, heavy and costly in high power supply systems.

The basic principle of the topology in Fig.2 is that the use of a feedback loop as shown is capable of increasing the equivalent capacitance for high frequencies. This is illustrated in **Fig.3** where one can see that, for the lower frequency end the original capacitance of C_o is effective, but for higher frequencies an increase in the capacitance value is possible depending on the used feedback loop, according to

$$Z_{act}(s) = \frac{U_F(s)}{I_{test}(s)} = \frac{1}{s \cdot C_o} \cdot \frac{1}{1 + G_{fb}(s)} \cdot \qquad (1)$$

With this equation it is seen that the capacitance in basically multiplied by the feedback gain G_{fb}. This characteristic is very important in this type of system, since the capacitance at low frequency should be as small as possible due to the limited earth leakage current.

III. STABILITY ANALYSIS AND DESIGNED FEEDBACK STRUCTURE

There are basically four strict requirements for the filter structure:

- The attenuation for high frequency needs to be higher than for a passive filter with the same components;
- The value of the capacitor (C_o) is limited due to the safety considerations (earth leakage currents);
- The 50/60 Hz and the low frequency harmonic components present in the voltage u_F are quite large when compared with the high frequency components. As a requisite they have to be very well attenuated in the feedback loop otherwise the amplifier output will be constantly saturated;
- The system has to be stable for a large range of source and mains impedances.

Once an active part is included in the topology, the natural stability achieved with only passive elements can not be further guaranteed and a careful study of the stability should be carried out. The study of possible gains in the feedback loop and the measurement/control structures that lead to higher stability margins is of great importance since the 50/60 Hz component demands for a quite high attenuation factor.

The use of Bode diagrams for the stability study is not sensible once the structures do not fulfill the requirement (steadily decrease of the open loop gain and phase curves) for a straightforward analysis by frequency domain plots. Therefore, the root locus analysis is the tool to be used.

As a starting point for the stability analysis of the proposed active filter the circuit of **Fig.4** is used where the reactive components consider the inductive characteristics of the mains and the mainly capacitive nature of the CM noise source.

The closed loop system can have its open loop transfer function (transmission loop) calculated by opening the loop at the output connection of the amplifier u_c. This is a logical step since the output impedance of the amplifier is expected to be much lower than the
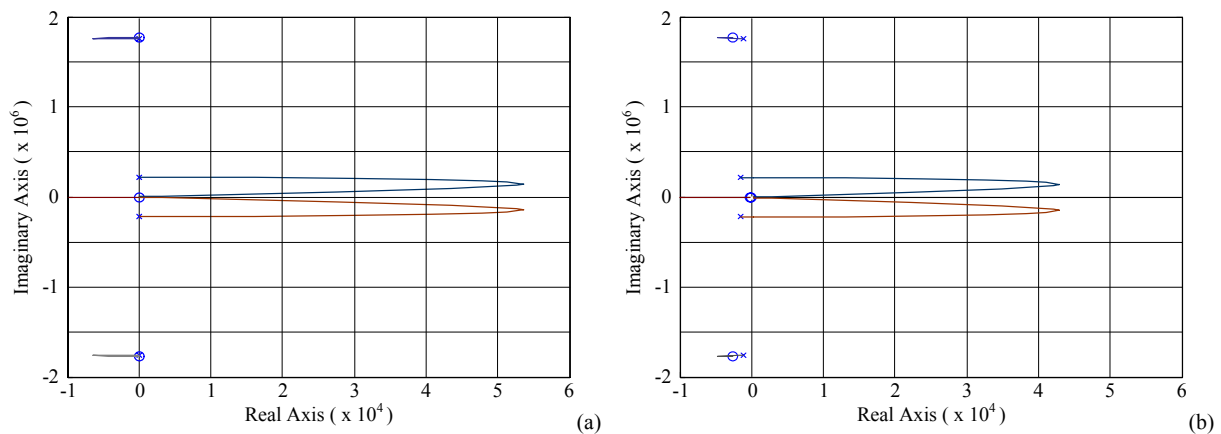
Fig.6: Root locus diagrams for the active filter plant for the parameters specified in Fig.5. **(a)** Root locus for a filter plant purely reactive. **(b)** Diagram illustrating the changes in the positions of the singularities due to the inclusion of parasitic resistive elements for the same filter plant.

input impedance of the output coupling capacitor C_o. By opening the loop as described, short-circuiting the voltage sources and assuming an operational amplifier with ideal characteristics, the system can have its stability analyzed through the circuit depicted in **Fig.5**(a), where the impedances $L_{CM,2}$ and Z_{mains} are summed to L_g and the impedances $L_{CM,1}$ and L_{source} to L_s. The feedback capacitance C_f is also part of the plant, since it adds a zero and changes the pole positions. With these considerations, the feedback variable of interest is the current i_F, which is multiplied by the impedance Z_f for the final shaping of the feedback loop. As an example, a bode plot from the considered plant, for the parameters given in Fig.5, is shown in Fig.5(b).

If no damping elements are considered, the root locus for the system of Fig.4 is plotted in **Fig.6**(a) from

$$\frac{I_F(s)}{U_c(s)} = \frac{s^3 L_g C_f C_o (s^2 C_s L_s + 1)}{s^4 L_g L_s (C_o + C_f) C_s + s^2 \left[L_g (C_o + C_f - C_s) + L_s C_s \right] + 1}. \quad (2)$$

A deeper analysis of this root locus plot shows that it characterizes a plant quite difficult to stabilize, presenting three zeros at the origin and four poles at imaginary axis. The stabilization of this plant can be done, for instance, if two poles are placed at low frequencies and a pair of zeros is placed at high frequencies. With this placement, a very large DC gain would have to be employed ($> 10^6$), which is not feasible due the characteristics of practical HF power amplifiers and would ruin the 50/60 Hz rejection. Other zeros/poles placement is possible, but would lead to a very complex feedback structure including complex zeros and poles. For this reason the proper modeling of the resistive elements of the circuit is of high importance, as it moves the plant singularities to the left half plane as shown in the root locus of Fig.6(b). With this, it is possible to employ simpler feedback structures, which can then properly reject the low frequency components, but will have their maximum HF gain limited.

As previously cited, a limited supply is to be used for the power amplifier and it is not desirable that the closed loop system tries to influence the circuit behavior at 50 Hz. For a single-phase system, it is necessary that the low frequency components of the measured voltage are highly reduced in the feedback loop. A value of approximately -40

dB attenuation for the 50 Hz component would mean that for a 300 V peak in the line to ground (PE) voltage, a peak voltage of 3 V appears in the output of the power amplifier. In this case a minimum attenuation of -50 dB at 50 Hz was chosen as a starting point.

Another specification is that the high frequency gain should be practically feasible with a low cost HF power amplifier. This specification matches also the gain limitation imposed by the plant characteristics. The actuator for the proposed system is a linear HF power amplifier G_{amp} presenting enough bandwidth in order to allow a good performance. A good model for such amplifier is a first order low pass with and a limited output swing due to the available supply voltage.

The most simple and desirable measurement technique is to use a high-pass filter. In the case at hand it is composed of two zeroes, one at the origin and the other above 10 kHz. This results in a high attenuation of the 50/60 Hz component. Poles at high frequency are placed in order to limit the high frequency gain. The final bandwidth of the feedback loop is set by the power amplifier limitations.
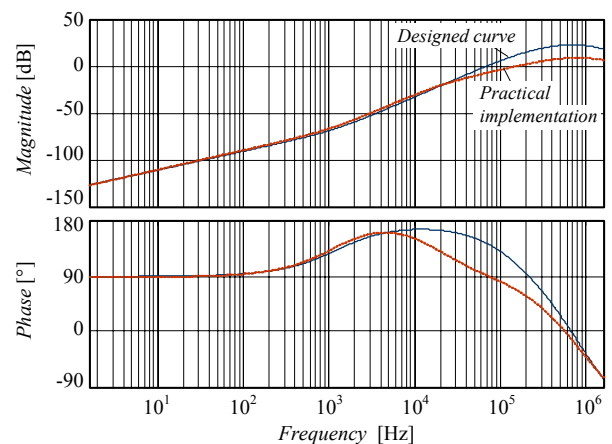

Fig.7: Bode diagrams for the designed feedback loop. The high frequency gain for the practical implementation was lowered due a non-ideal behavior of the HF power amplifier not modeled.
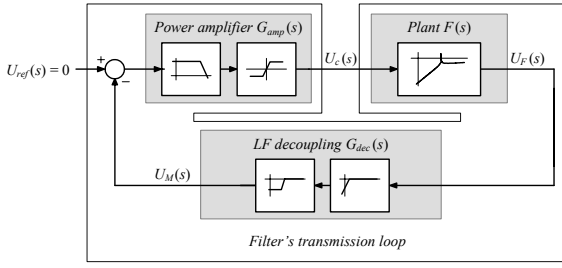
Fig.8: Block diagram of the proposed system.

The designed feedback loop, including the capacitance C_f can be observed in Fig.7, where a curve for the designed loop and another curve for the actual performance of the finally implemented system are shown. The reason for the HF gain reduction at high frequencies is the maximum slew-rate of the implemented power amplifier, which results in a 180° phase-shifting (two complex conjugate poles) that prevented higher gains to be applied in practice. This reduction in the HF gain limits the final achievable attenuation increase.

The final control oriented block diagram of the designed system is presented in **Fig.8** from where the final root locus diagram of the transmission loop is plotted in **Fig.9**(b) for the circuit of Fig.9(c), while its bode plot is presented in Fig.9(a). The inductors are modeled here as a constant inductance in series with a resistance, allowing the system stability to be analyzed with linear systems mathematical tools. With the previously shown feedback structure, the determining part of the root locus is the region close to the origin, which includes the low frequency zeros and the dominant complex poles. The design ensures that large values of mains and noise source impedances can be employed, as well as a very wide range of noise source capacitance. Furthermore, it is in a way that minimum values for the inductors $L_{CM,1}$ and $L_{CM,2}$ have to be employed which practically decouple the influence of the external impedances on the stability of the system.

IV. PRACTICAL IMPLEMENTATION OF THE ANALYZED FILTER

A three-phase filter employing the presented feedback structure was built in order to test the presented mathematical models. The filter sc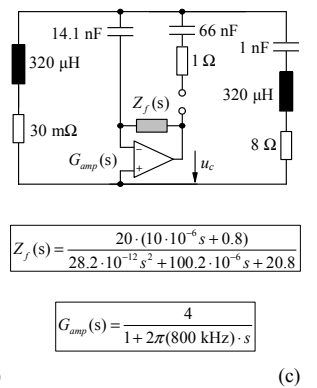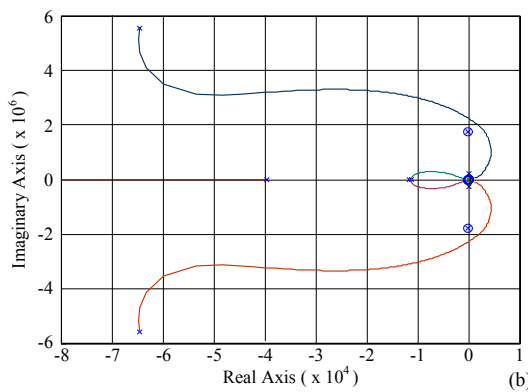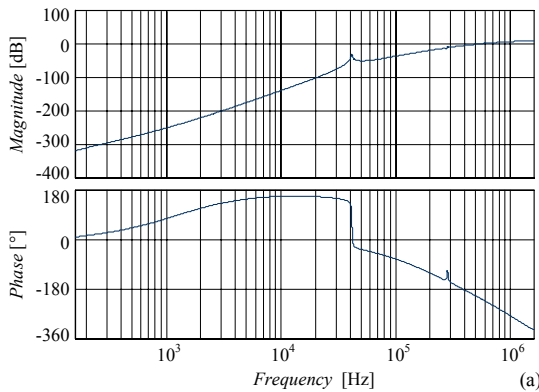hematics are presented in **Fig.11** and the main components are specified in **Table I**. The filter employs inductors built with nanocrystalline cores (VAC Vitroperm 500F), which have a highly resistive behavior at high frequencies, helping to ensure high impedances at high frequencies, a well damped self resonance and good thermal stability. The inductors are modeled taking the complex permeability curves from the manufacturer and the parallel capacitances are modeled as in [21]. The capacitors are modeled using their datasheet information including their equivalent series resistance and inductance.

In hand of this modeling, the filter insertion loss (50 Ω input / 50 Ω output measurement) curves for the designed filter were calculated as shown in **Fig.10**, where the curve for the filter without feedback can be compared with real measurement data (indicated by crosses) and a good agreement is observed, except for a resonance at approximately 20 MHz. Based on the modeled components two simulations were performed and their results are also presented in Fig.10. The first simulation (middle trace in Fig.10) is the filter insertion loss if a band-limited amplifier is used, showing that an increase in the attenuation is observed up to the amplifier's frequency limitation. The last simulation is for an infinite bandwidth amplifier. The potential for such systems is clear and with larger amplifiers bandwidth, better performance is observed.
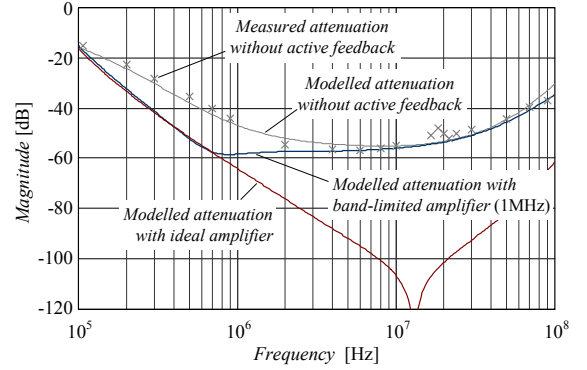

Fig.10: Insertion loss curves (50 Ω input / 50 Ω output measurement) for different feedback structures. The crosses represent real measurements in the built filter board with no active feedback, while the top line shows the insertion loss for the mathematically modeled filter. The middle curve depicts the expected behavior when utilizing an active feedback, which makes use of a band-limited power amplifier, while the lower curve shows the performance with the circuit employing an infinite bandwidth amplifier.
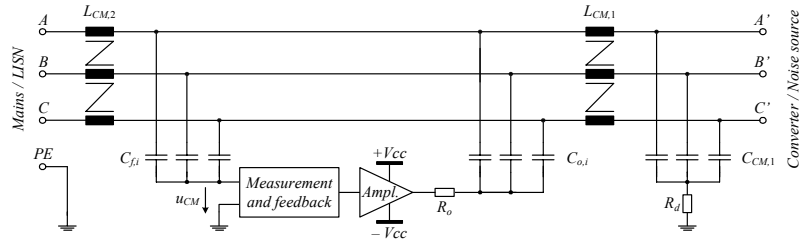

$$Z_f(s) = \frac{20 \cdot (10 \cdot 10^{-6} s + 0.8)}{28.2 \cdot 10^{-12} s^2 + 100.2 \cdot 10^{-6} s + 20.8}$$

$$G_{amp}(s) = \frac{4}{1 + 2\pi(800 \text{ kHz}) \cdot s}$$

Fig.9: Final diagrams for the designed system. **(a)** Bode plots for the modeled transmission loop including resistive elements and two high frequency poles modeling the power amplifier. **(b)** Root locus diagram for the designed system. **(c)** Circuit used for the transmission loop calculations and the relevant functions.

Fig.11: Circuit schematic for the designed filtering system. Components are specified in Table I.

TABLE I – SELECTED COMPONENTS FOR THE ACTIVE FILTER PROTOTYPE.

Component	Specification
$C_{f,i}$	Y2 SMD Capacitor, Murata X7R Series GC 4.7 nF – 250Vac
$C_{o,i}$	Y2 Capacitor , Epcos MKP B81122 22 nF – 250Vac
$C_{CM,i}$	Y2 SMD Capacitor, Murata X7R Series GC 1nF – 250Vac
$L_{CM,1}$	Vaccuumschmelze VAC VITROPERM 500F T6000-6-L2012-W498 – OD(12.5) ID(10) H(5) mm N = 3 x 3 turns, $\varnothing$ 1 mm²
$L_{CM,2}$	Vaccuumschmelze VAC VITROPERM 500F T6000-6-L2012-W498 – OD(12.5) ID(10) H(5) mm N = 3 x 4 turns, $\varnothing$ 1 mm²

Based on the promising simulation results a prototype was built using the structure of **Fig.11**. The filter is rated for 10A/400V/50Hz. A discrete HF power amplifier as shown in **Fig.12** was designed and built for a system being fed with a ±30 V external power supply. The amplifier is built with conventional SMD components and presents a -3dB bandwidth of approximately 1 MHz. A photograph of the prototype is shown in **Fig.13**.

Fig.12: Schematic of employed linear HF power amplifier. The topology is selected aiming for low implementation costs.
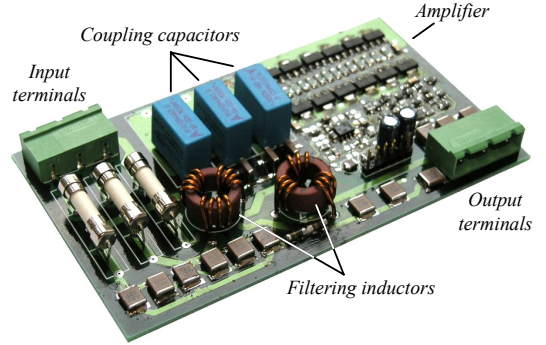

Fig.13: Three-phase filter prototype photograph (120 x 70 x 17 mm³).

The first step in the prototype testing was to analyze the system stability under different source and load impedances. Inductors with ferrite cores of 1 mH and 6 mH, and inductors with nanocrystalline cores of 4.2 mH and 12 mH (measured at 1 kHz) were used as artificial mains and/or source impedances. On the noise source side, capacitors in the range of 10 pF up to 10 µF were employed. Short-circuiting of the filter inputs to PE was also tested. For all these impedances the filter presented stable behavior.

Attenuation measurements were also performed employing different source and load impedances. **Fig.14**(a) presents the measurement for a 8 Ω input impedance and a 50 Ω output for the filter structure with and without (C_f and $C_{o,i}$ shorted to PE) active feedback. The same measurements were repeated for a 4.2 mH source impedance and the results are presented in Fig.14(b), showing the increase in the filter attenuation in the range of 100 kHz to 1 MHz, where the amplifier bandwidth ends.

The last performed test made use of a square wave generator as noise source in series with a 400 pF SMD capacitor. As load, a four-line 50Ω/50µH V-network LISN was used and its output connected to an EMC test receiver. Measurements with and without filter are pre-
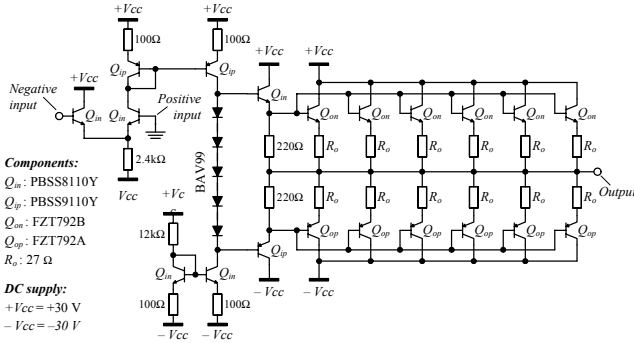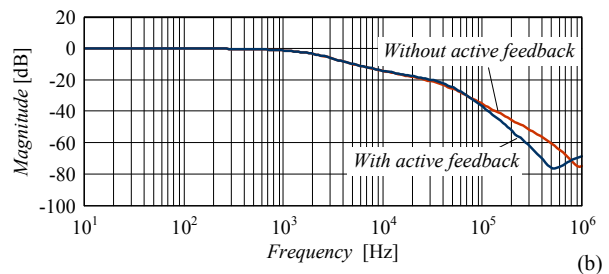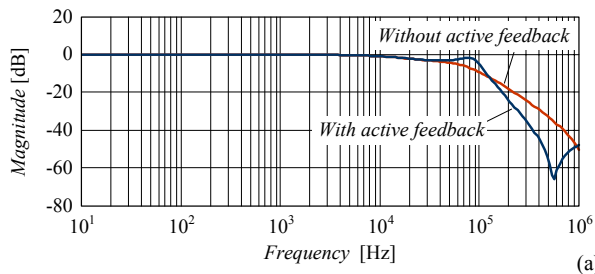

(a)

(b)

Fig.14: Measured attenuation curves for a load impedance of 50 Ω. **(a)** Performance for the designed filter (cf. Fig.13) with a source impedance of approximately 8 Ω. **(b)** Designed filter with source impedance of approximately 4.1 mH (measured at 1 kHz).

sented in **Fig.15**. For the measurement with the active feedback, it is clear that higher attenuation is achieved up to 1 MHz. At 2 MHz a resonance in the amplifier circuit due to the distortion caused by its slew-rate limitation is seen, what causes higher emission levels than those of the filter without feedback. In the higher frequency range the same conducted emission levels are seen.
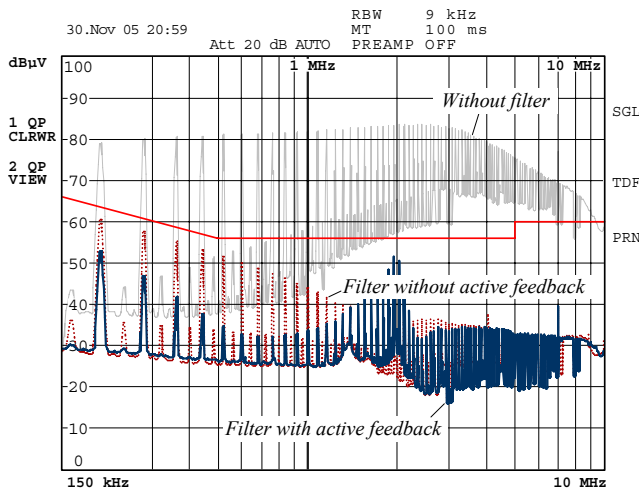

Fig.15: Conducted emission measurements performed employing a square wave generator switching at 40 kHz with a rise/fall time around 30 ns in series with a capacitance of approximately 400 pF. Upper trace shows the emission levels without a filter. Dashed trace shows the measurement result with no active feedback. Third trace presents the results when the electronic feedback is active.

V. CONCLUSIONS AND OUTLOOK

This paper proposes an implementation strategy for an active, i.e. HF amplifier based CM filter for off-line converter systems. For such a system the low frequency (50/60 Hz) attenuation in the feedback loop is of high importance in order not to saturate the amplifier, but limits its operating frequency range. A literature survey is carried out for identifying the possible filter structures and presenting the critical issues and main advantages for the selected approach. The designed filter is based on capacitive coupling for both measurement and actuation preventing the use of HF transformers. The filter function is explained in detail and a stability analysis procedure is presented which is carried out with reference to root locus diagrams and simplified circuit models. A feedback design for the selected filter topology is proposed, which fulfills the stability requirements for the system and allows for higher filter attenuation and/or smaller passive filter components. Based on the simulation and practical results, this system presents potential for application in a practical system. Due to the highly reactive nature of the filter structure, high gain for the higher frequency end is limited, but the use of a higher bandwidth amplifier would allow better results. Based on the potential of this technique, other types of feedback structure are also to be researched and are the aim of future works. Furthermore, the protection of the HF amplifier stage in case of voltage surges or bursts will be analyzed in detail as it is a main determining factor for the applicability of active filters in off-line applications. The analysis of the possibility of series and par-

allel connections of active filter cells shall be also analyzed.

REFERENCES

[1] J. Walker, "Designing Practical and Effective Active EMI filters," in *Proc. of Powercon 11*, vol. I-3, 1984, pp. 1-8.

[2] L. LaWhite and M.F. Schlecht, "Active Filters for 1-MHz Power Circuits with Strict Input/Output Ripple Requirements", *IEEE Trans. Power Electron.*, vol. 2, pp. 282-290, Oct. 1987.

[3] L. LaWhite and M.F. Schlecht, "Design of Active Ripple Filters for Power Circuits Operating in the 1-10 MHz Range", *IEEE Trans. Power Electron.*, vol. 3, no. 3, pp. 310-317, Jul. 1988.

[4] T. Farkas and M.F. Schlecht, "Viability of Active EMI Filters for Utility Applications", in *Proc. IEEE APEC'92*, 1992, pp. 803-813.

[5] K. Hironobu, F. Katsumi, "Active Filter", Japanese Patent 087973, 2003.

[6] Y.-C. Son and S.-K. Sul, "A New Active Common-Mode EMI Filter for PWM Inverter", *IEEE Trans. Power Electron.*, vol. 18, no. 6, pp. 1309-1314, Nov. 2003.

[7] E.V. Larsen, R. Delmerico, "Hybrid Active Power Filter with Programmed Impedance Characteristics", U.S. Patent 5737198, 1998.

[8] B. Pelly, "Active Common Mode Filter Connected in A-C Line", U.S. Patent 6690230, 2004.

[9] S. Ogasawara, H. Ayano and H. Akagi, "An Active Circuit for Cancellation of Common-Mode Voltage Generated by a PWM Inverter," *IEEE Trans. Power Electron.*, vol. 13, no. 5, pp. 835-841, Sept. 1998.

[10] S. Ogasawara and H. Akagi, "Circuit Configurations and Performance of the Active Common-Noise Canceller for Reduction of Common-Mode Voltage Generated by Voltage-Source PWM inverters", in *Proc. IEEE IAS'2000*, vol. 3, pp. 1482-1488.

[11] A.C. Chow and D.J. Perreault, "Active EMI filters for automotive motor drives", in *Proc. Power Electronics in Transportation 2002*, 2002, pp. 127-134.

[12] Y. Kanehara, "Noise Filter", Japanese Patent 244770, 2001.

[13] J. Honda, "Active EMI Filter having no Inductive Current Sensing Device", International Patent 109896, 2004.

[14] J. Honda, "Active EMI Filter", International Patent 001927, 2004.

[15] D.Y. Lee and B.H. Cho, "Design of an Input Filter for Power Factor Correction (PFC) AC to DC Converters Employing an Active Ripple Cancellation", in *Proc. IECEC 96*, 1996, vol. 1, pp. 582-586.

[16] M. Zhu, D.J. Perreault, V. Caliskan, T.C. Neugebauer, S. Guttowski and J.G. Kassal, J.G., "Design and Evaluation if an Active Ripple Filter with Rogowski-Coil Current Sensing", in *Proc. IEEE PESC'99*, 1999, vol. 2, pp. 874-880.

[17] J. Dumas, B. Lanoue and B. Tahhan, "Active analog power filters provide solutions for EMC and EMI", in *Proc. IEEE APEC'04*, 2004, vol. 2, pp. 675-680.

[18] B. Pelly, "Active Filter for Reduction of Common Mode Current", U.S. Patent 6636107, 2003.

[19] J.R. Nicholson and J.A. Malack, "RF lmpedance of Power Lines and Line lmpedance Stabilization Networks in Conducted Interferences Measurement", *IEEE Trans. Electromagnetic Compatibility*, vol. 15, no. 2, pp. 84-86, May. 1973.

[20] J.P. Rhode, A.W. Kelley and M.E. Baran, "Line impedance measurement: a nondisruptive wideband technique", in *Proc. IEEE IAS '95*, 1995, vol. 3, pp. 2233-2240.

[21] A. Massarini, A., Kazimierczuk, M.K. and Grandi, G., "Lumped parameter models for single- and multiple-layer inductors", in *Proc. IEEE PESC'96*, 1996, pp. 295-301.